



ELSEVIER

Available online at www.sciencedirect.com

Infection Prevention in Practice

journal homepage: www.elsevier.com/locate/ijip

Investigations into the efficacy of a novel extubation-aerosol shield: a cough model study[☆]

Gen Hasegawa^{a,*}, Wataru Sakai^a, Tomohiro Chaki^a, Shunsuke Tachibana^a, Atsushi Kokita^a, Takenori Kato^b, Hidekazu Nishimura^c, Michiaki Yamakage^a

^a Department of Anaesthesiology, Sapporo Medical University School of Medicine, Sapporo, Japan

^b Kato Koken, Isehara, Japan

^c Virus Research Centre, Clinical Research Division, Sendai Medical Centre, Sendai, Japan

ARTICLE INFO

Article history:

Received 12 August 2021

Accepted 30 November 2021

Available online 4 December 2021

Keywords:

COVID-19

Aerosol-generating procedure

Airway management

Coronavirus

Mechanical ventilation

Tracheal extubation



SUMMARY

Background: Physicians have had to perform numerous extubation procedures during the prolonged coronavirus disease 2019 (COVID 19) pandemic. Future pandemics caused by unknown pathogen may also present a risk of exposure to infectious droplets and aerosols. **Aim:** This study evaluated the ability of a newly developed aerosol barrier, "Extubation-Aerosol (EA)-Shield" to provide maximum protection from aerosol exposure during extubation via an aerosolised particle count and high-quality visualisation assessments.

Methods: We employed a cough model having parameters similar to humans and used micron oil aerosol as well as titanium dioxide as aerosol tracers. Aerosol barrier techniques employing a face mask (group M) and EA-Shield (group H) were compared.

Findings: The primary outcome was the difference in the number of particles contacting the physician's face before and after extubation. The maximum distances of aerosol dispersal after extubation were measured as the secondary outcomes. All aerosolised particles of the two tracers were significantly smaller in group H than in group M ($p < 0.05$). In addition, the sagittal and axial maximum distances and sagittal areas of aerosol dispersal for 3, 5, and 10 s after extubation were significantly smaller in group H than in group M ($p < 0.05$).

Conclusion: This model indicates that EA-Shield could be highly effective in reducing aerosol exposure during extubation. Therefore, we recommend using it as an aerosol barrier when an infectious aerosol risk is suspected.

© 2021 The Authors. Published by Elsevier Ltd on behalf of The Healthcare Infection Society. This is an open access article under the CC BY-NC-ND license (<http://creativecommons.org/licenses/by-nc-nd/4.0/>).

[☆] Presentation: This study, in part, was presented as a poster at the 68th Annual Meeting of the Japanese Society of Anesthesiologist, Web, Japan, June 5th- July 9th, 2021.

* Corresponding author. Address: Department of Anaesthesiology, Sapporo Medical University School of Medicine, 291, South 1, West 16, Chuo-ku, Sapporo, Hokkaido, Japan. Tel.: +81 80-4603-7803.

E-mail address: minamoto05@gmail.com (G. Hasegawa).

Introduction

Physicians must pay attention to droplet and aerosol exposure not only during intubation but also during extubation, which is a droplet and aerosol-generating procedure [1]. During a prolonged pandemic, such as that caused by the severe acute respiratory syndrome coronavirus 2 (SARS-CoV-2) virus,

<https://doi.org/10.1016/j.infpip.2021.100193>

2590-0889/© 2021 The Authors. Published by Elsevier Ltd on behalf of The Healthcare Infection Society. This is an open access article under the CC BY-NC-ND license (<http://creativecommons.org/licenses/by-nc-nd/4.0/>).

physicians have to perform numerous extubation procedures that have a risk of infectious droplet and aerosol exposure. SARS-CoV-2 can be transmitted even by asymptomatic people through droplets and aerosols, and personal protective equipment (PPE) cannot completely protect against their spread [2,3]. Anaesthetists and intensivists are at low risk of SARS-CoV-2 infection, possibly due to well-ventilated working environment and the use of high-performance PPE [4]. However, in reality, aerosol procedures must be performed without sufficient air conditioning and PPE, when the distance between hospital beds is insufficient. Protection against viral infections during intubation, outside of a well-equipped environment has not yet been established. Pathogens including SARS-CoV-2, SARS-CoV, and influenza virus can be transmitted during aerosol-generating procedures [5]. Mass-producible and single-use aerosol barriers are needed during aerosol-generating procedures when there is a shortage of protective equipment. Several guidelines do not provide clear evidence of using aerosol barriers to protect against droplet infections during extubation [6–8]. Although several aerosol barriers have been developed for use, during these procedures [9–13], they have not been fully tested to check the dispersal of aerosol particles of a size that would allow them to remain infectious. Although one guideline has recommended using a face mask as an aerosol barrier during extubation [14], its effectiveness against aerosol protection is unclear. However, the dispersal of aerosols cannot be perceived visually by the naked eye. Protective methods need to be based on evidence of aerosol dispersal. Moreover, it is necessary to establish a safer method of extubation that can be performed under adverse conditions, including inadequate air conditioning and insufficient PPE.

We have developed an aerosol barrier termed “Extubation-Aerosol (EA)-Shield” (Figure 1) to protect physicians and medical staff against aerosol exposure during extubation. The barrier is mass-producible at a low cost and can be manufactured and used in developing countries. With the EA-Shield, emergency airway management after extubation, including mask ventilation and oral suctioning, can be performed without modification.

This study assessed the ability of EA-Shield to provide effective protection against aerosol exposure during extubation that was performed using aerosolised particle counting and high-quality visualisation techniques.

Materials and methods

Study design

This study did not involve human subjects as well as patient consent or the approval of internal review boards. This was an analytical and observational *in vitro* study.

EA-Shield

The EA-Shield can be made from a common 120-l plastic bag (1 m × 1.2 m), with all edges closed (Figure 1A, C–F, Video S1). The EA-Shield has one large elliptical hole on the lower layer (patient’s side) and four small holes with double-sided tape on the upper layer for each face mask, endotracheal tube, oral suction tube, and nasogastric tube. It was designed such that after extubation, the airway can be secured with a face mask

through the slit in the shield, and suction can be performed with a suction tube.

Supplementary data related to this article can be found at <https://doi.org/10.1016/j.infpip.2021.100193>.

Environment and procedures

All experiments and calculations were performed after confirming adequate ventilation in the laboratory. Before each experiment, the number of atmospheric particles was determined using an airborne particle counter (P8-306, Airy Technology Japan Ltd, Kanagawa, Japan) and checked within the acceptable range of standard values according to our preliminary data (Table S1).

A high-fidelity AirSim Patient Simulator (Trucorp, Belfast, Northern Ireland), generated from the computed tomography scan of a human subject (65-year-old Caucasian, weight 62 kg), was used (Figure 1B). In addition, an air blower (Air blower, Kato Koken, Isehara, Japan) was used as a cough simulator, and the vinyl chloride pipe connecting the trachea of the mannequin to this air blower was surrounded by clay to prevent air leakage, thereby strengthening it against the jet pressure of the cough simulator. The air blower was adjusted to create cough patterns resembling those of humans (Table S1).

We used titanium dioxide (Tree of Life, Tokyo, Japan) and micron oil aerosol (Kato Koken) as the aerosol model and tracer, respectively. Titanium dioxide as an aerosol has a wide range of particle sizes (0.07–11 µm, $D_{50} = 3.92$ µm), that were measured with a particle counting device (LA-950, Horiba, Kyoto, Japan). Micron oil aerosol ($D_{50} = 10$ µm), generated by PS-2006 (Dainichi, Niigata, Japan), has been used for visualisation experiments in the field of fluid mechanics owing to its ability to track airflow. In each experiment, titanium dioxide (0.25 g) and micron oil aerosol (300 ml) were placed into the mouth of the patient simulator without leakage, before firing the air blower. Before each procedure, the mannequin was cleaned from inside with an air blower to remove any remaining tracers.

The intake port of an airborne particle counter (P8-306) was positioned just beside the head of the physician at head height (75 cm above the head of the simulated patient). This device counts airborne particles with sizes of 0.3, 0.5, 1.0, 2.5, 5.0, and 10 µm, for 1 min. The flow rate of our airborne particle counter was 2.83 l/min, with detection of ambient air occurring in 1 s sweeps.

We used two types of light sources: white LED light (wavelength, 430–700 nm; 90 W) (Kato Koken) to assess the spatial aerosol spread and a thin green laser light sheet generated by a YVO4 laser (wavelength, 532 nm; 2,000 mW) (Kato Koken) to assess the sagittal and transverse aerosol spread from the mannequin’s mouth and to measure the hydrodynamic outcomes. All coughing jet plume images were captured by a camera specialised for visualising fine particles (PV2, Kato Koken) with an optical resolution of $2,048 \times 1,536$ pixels per video frame. The maximum speed was 120 fps. All particle image velocimetry system images were captured using a high-speed camera (Kato Koken) with an optical resolution of 640×480 pixels per video frame. The maximum video frame speed was 8,000 fps.

The white LED light was placed 2 m caudal to the mouth of the mannequin. Video cameras were placed on the side and 45° diagonally upwards. The green slit-sheet light and video

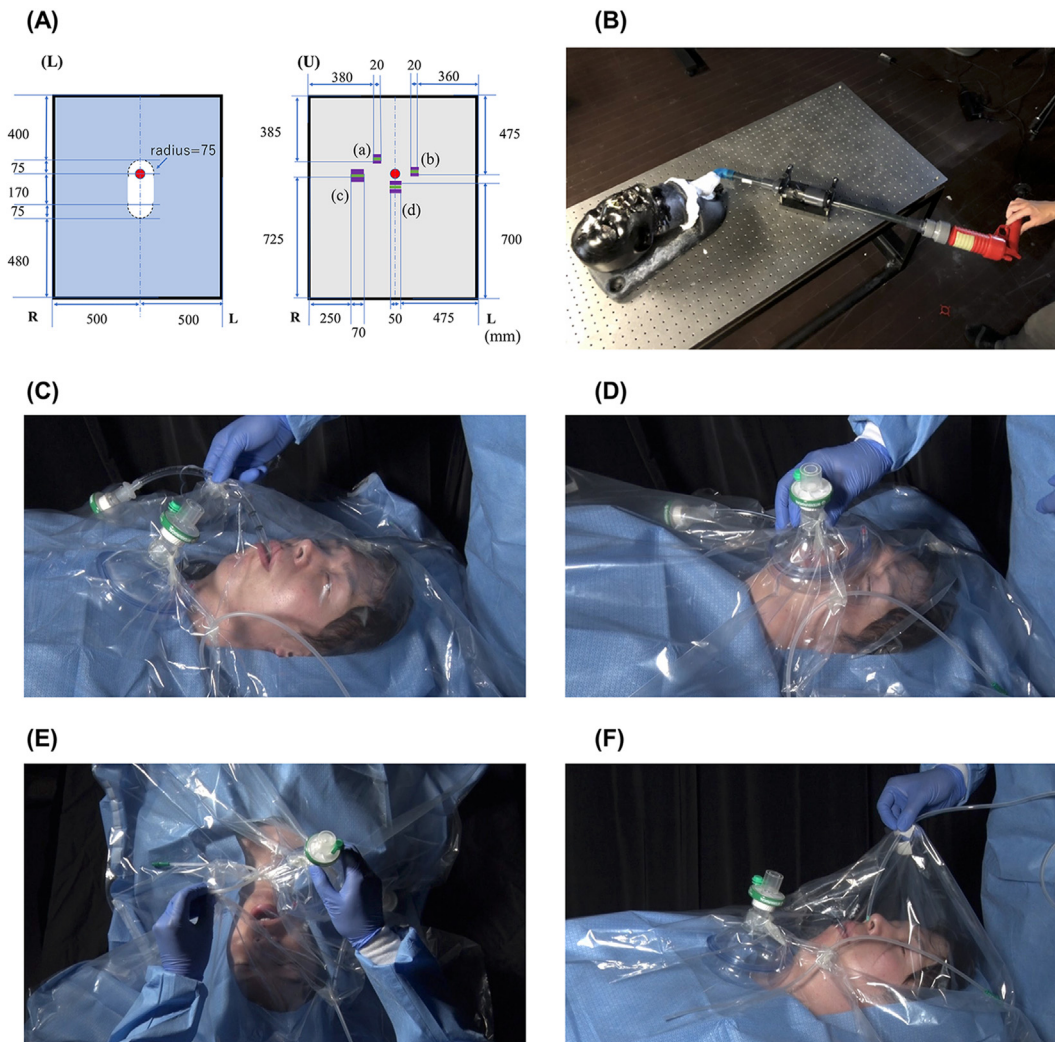


Figure 1. Experimental methods and the method for constructing the Extubation-Aerosol (EA)-Shield. (A) EA-Shield and method for constructing an EA-Shield from a 120-L plastic bag. The opening of the plastic bag is closed with tape. The numeric units of the figure are in mm. (B) The airway and cough simulator. (C) Holes are made for each endotracheal tube, face mask (D), suction (E), and nasogastric tube (F) and are closed with a double-sided tape. Clear layer, upper layer of the plastic bag; blue layer, lower layer of the plastic bag; purple lines, double-sided tape; red circle, patient's mouth. (U) upper layer, (L) lower layer, (a) upper slit for nasogastric tube, (b) left slit for suction, (c) right slit for endotracheal tube, (d) lower slit for a face mask; R right side, L left side.

camera were placed orthogonally. To prevent reflection of light that could lead to errors in the video graphic measurements, the physician dressed completely in black, and the mannequin was painted black by a professional painting company (Ihara Paint, Hokkaido, Japan). The image analysis was based on the principle that the intensity of the scattered light is proportional to the particle concentration. The area of scattered particles illuminated with the green slit-sheet light was recorded and analysed using image software (Particle Viewer, Kato Koken, Japan). The reference area was set at $2,048 \times 1,536$ pixels to 136.7×102.4 cm.

We placed an 8.0-mm tube (Hi-Contour Oral/Nasal Tracheal Tube Cuffed; Covidien, Dublin, OH) into the trachea of the mannequin and fixed it at a depth of 22 cm in the right corner of the mouth. The timing of extubation was defined as the withdrawal of the endotracheal tube from the corner of the mouth to a depth of 16 cm and the position of the glottis. The firing

from the air blower was synchronised with the moment of extubation, to ensure a constant timing of the simulated cough during all experiments.

Aerosol barrier during extubation

Two different aerosol barrier techniques were used during extubation:

- i) Mask-over-tube extubation technique (face mask method: group M) [10].

In this method, the tracheal tube was extubated while using the face mask to prevent aerosol dispersal caused by the patient's cough. This technique is recommended in published guidelines as an effective aerosol barrier method [14].

ii) Extubation with EA-Shield (Hasegawa method: Group H)

The Hasegawa method requires only an EA-Shield. The details of the Hasegawa method are presented in Table S1.

Study outcomes

The primary outcome was the difference in the number of particles before and after extubation as aerosol exposure to the physician. The baseline values are listed in Table SII. In

addition, the following secondary outcomes were verified using high-quality video images during extubation.

i) Sagittal and axial distances of aerosol spread in videography taken from the mannequin's side with the green laser sheet for 3, 5, and 10 s after the air blower fired. ii) Sagittal area of aerosol spread in videography taken from in front of the mannequin with the green laser sheet, for 3, 5, and 10 s after the air blower fired. iii) Vectors of aerosol spread in videography were taken from the mannequin's side using a green laser sheet. Titanium dioxide was used as a tracer to measure secondary outcomes.

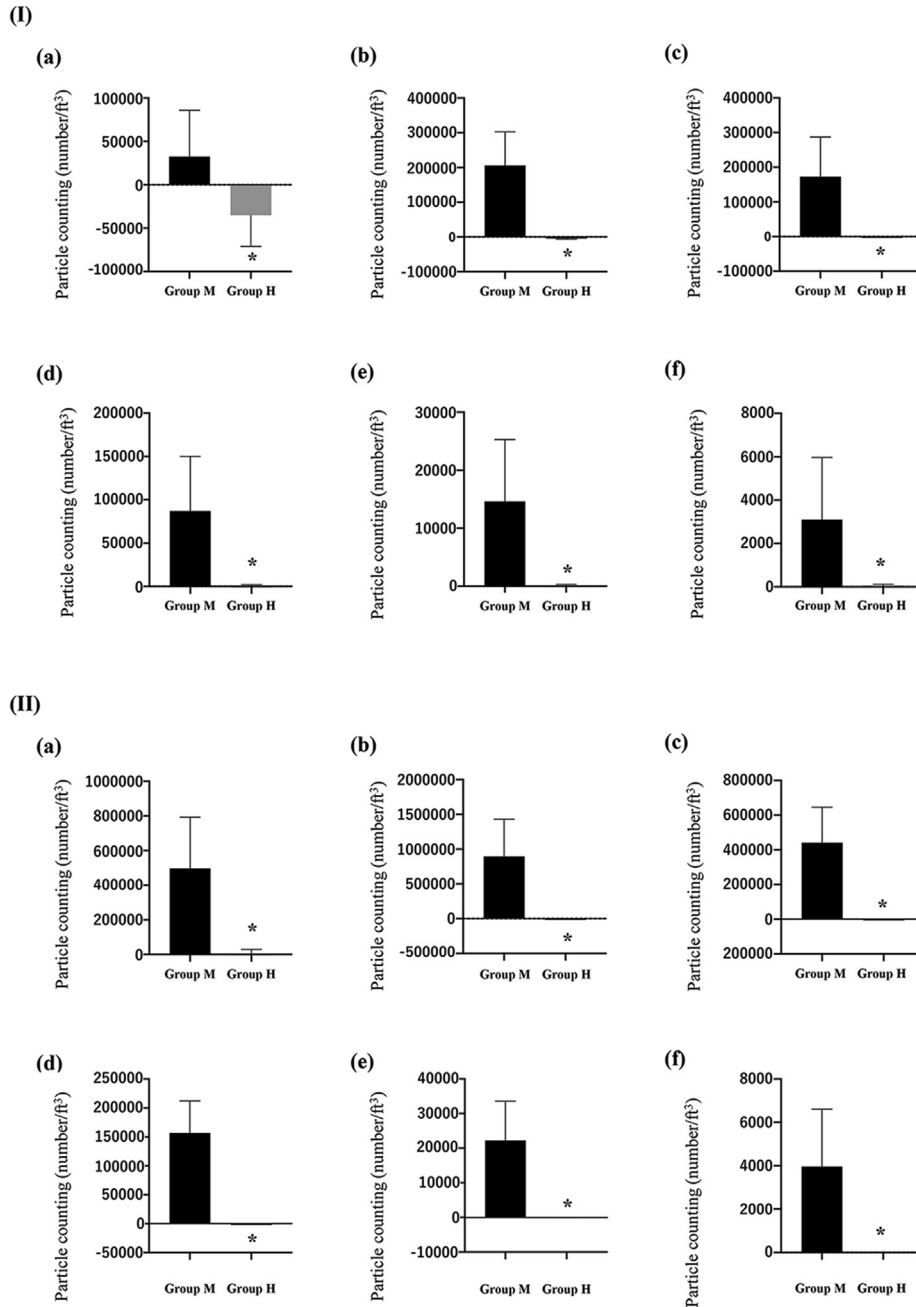


Figure 2. Summary of particle counting for micron oil aerosol and titanium dioxide. All micron oil aerosol and titanium dioxide particles were significantly smaller in group H than in group M. (I) Results of particle counting for micron oil aerosol. (II) Results of particle counting for titanium dioxide. Particles with diameters of (a) 0.3 μm, (b) 0.5 μm, (c) 1.0 μm, (d) 2.5 μm, (e) 5.0 μm, and (f) 10 μm. *p < 0.05.

Statistical analysis

The Shapiro-Wilk test was used to determine whether the data were normally distributed. Normally distributed variables are shown as the mean (SD), and non-normally distributed data are shown as median and interquartile range (IQR). Data were analysed using the unpaired t-test or Mann-Whitney U test. Statistical significance was set at $p < 0.05$. All statistical analyses for this study were performed using GraphPad Prism 8.0 (GraphPad Software, La Jolla, CA). Vector analysis was performed using software FlowExpert2D2C (Kato Koken, Isehara, Japan).

According to our preliminary study of total particle counts, delta = 3,658,720 and SD = 1,946,610 represented significant differences (Table SIII). Sample sizes were calculated using R. version 3.5.3, with $\alpha = 0.05$, and $1-\beta = 0.8$, revealing that five samples were required in each group.

Results

All aerosolised particles of micron oil aerosol and titanium dioxide were significantly smaller in group H than in group M. The sizes of all aerosolised particles of both tracers in group H were within the baseline range. A summary of the primary outcomes is shown in Figure 2 and Tables SIV and SV.

Sagittal maximum distances of aerosol dispersal at 3, 5, and 10 s after the cough simulation were significantly smaller in group H than in group M. The axial maximum distances of aerosol dispersal for 3, 5, and 10 s after the cough simulation were also smaller in group H than in group M. The results of the sagittal and axial maximum distances of aerosol dispersal are presented in Table I.

The sagittal maximum areas of aerosol dispersal for 3, 5, and 10 s after the cough simulation were significantly smaller in group H than in group M. All results for the area of aerosol dispersal in group H were within the baseline range. The results are presented in Table I.

In the sagittal and axial videography with the green laser sheet (two-dimensional assessment from two directions), in group H, aerosolised particles were not observed after the cough simulation. In group M, aerosolised particles were expelled to the right of the mannequin, and they travelled a distance of 40 cm, 1 s after the cough simulation. The particles then moved in the left direction owing to the weak airflow in the experimental room. At 4 s after the cough simulation, the aerosolised particles travelled a distance of 50 cm in the caudal direction. Ten seconds after the cough simulation, the aerosolised particles covered the area around the physician and reached the roof of the experimental room. The results are summarised in Figures 3 and 4, as well as Video S2.

Supplementary data related to this article can be found at <https://doi.org/10.1016/j.infpip.2021.100193>.

On videography using white LED light (three-dimensional assessment), in group H, aerosolised particles were not observed after the cough simulation. In group M, aerosolised particles were expelled to the right of the mannequin, and they initially spread to the right side. At 4 s after the cough simulation, the particles surrounded the physician and reached the roof of the experimental room. A summary of the results is provided in Figures 3 and 4, as well as Video S2.

The maximum wind speed around the face of the mannequin determined by particle image velocimetry was 12.7 ± 1.72 m/s in group M. In group H, wind was not recorded during extubation. In group M, videography showed that the turbulent wind

Table I
Results of particle imaging velocimetry

Time after the cough	Group M (n=5)	Group H (n=5)	Hodges-Lehmann estimator	95% confidence interval	P-value
Sagittal Maximum Distance					
3 s (mm)	472 [445 to 488]	0 [0 to 0]	472	228 to 494	0.008
5 s (mm)	527 [521 to 620]	0 [0 to 0]	527	192 to 652	0.008
10 s (mm)	888 [744 to 895]	0 [0 to 0]	888	570 to 964	0.008
Axial Maximum Distance					
3 s (mm)	418 [415 to 438]	0 [0 to 0]	418	353 to 443	0.008
5 s (mm)	430 [408 to 486]	0 [0 to 0]	430	307 to 511	0.008
10 s (mm)	572 [507 to 637]	0 [0 to 0]	572	506 to 648	0.008
Sagittal Maximum Area					
3 s (mm ²)	9170 [4388 to 9568]	0.894 [0.894 to 2.235]	9567	4387 to 149695	0.011
5 s (mm ²)	12772 [7431 to 13638]	1.788 [1.788 to 5.812]	13633	7429 to 22129	0.012
10 s (mm ²)	22080 [6894 to 22244]	1.788 [1.788 to 1.789]	22078	4712 to 55419	0.011
Maximum velocity of aerosol dispersal during extubation					
	Group M (n=5)	Group H (n=5)			
Maximum velocity (m/s)	12.7 (1.72)	NA			

Sagittal and axial maximal distances and sagittal maximum areas 3, 5, and 10 s after the cough simulation and the maximum velocity of wind around the face of the mannequin were determined using a particle imaging velocimetry system. In group H, all sagittal and axial maximum distances were zero, but the maximum area in this group was not zero because some aerosolised particles were observed within the baseline range in the experimental room. The sagittal and axial maximum distances and sagittal maximum areas in group H were significantly smaller than those in group M. The axial maximum area could not be assessed because of the light reflection. In group H, wind was not observed around the face of the mannequin; therefore, maximum velocity could not be detected using the particle image velocimetry system. In group M, the wind speed around the face of the mannequin was higher than the cough speed (10 m/s) around the mouth of the mannequin because of the acceleration of wind speed in the space between the face mask and the face of the mannequin.

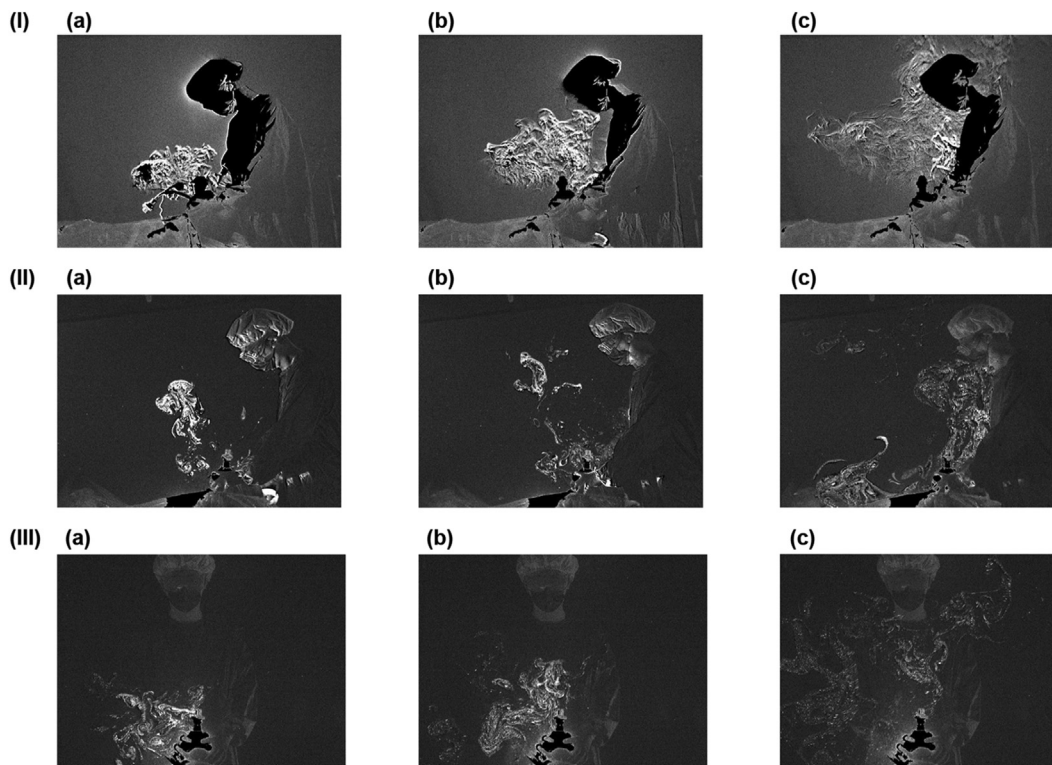


Figure 3. Photography of aerosol dispersal at 3, 5, and 10 s after the cough simulation with white LED light and green slit-sheet light in group M. (I) Photography with white LED light (three-dimensional assessments), (II) photography with green slit-sheet light in a sagittal view, and (III) photography with green slit-sheet light in an axial view (two-dimensional assessment from two directions). (a) Aerosol dispersal is shown at 3 s, (b) 5 s, and (c) 10 s after the cough simulation. Aerosol dispersal started from the right side of the mannequin and reached the physician's face. At 10 s after extubation, aerosolised particles had surrounded the physician's face.

emerged from the space between the face mask and the face of the mannequin in the straight right direction. A summary of the results is presented in [Figure 5](#) and [Table 1](#).

Discussion

The results of particle counting and the distance and area of aerosol dispersal in group H were all within the baseline range, indicating that EA-Shield could significantly prevent exposure of the physician to the aerosol particles (0.3–10 μm in size). These important results were supported by high-quality videography. The results of particle image velocimetry revealed that EA-Shield could also prevent wind generation as a result of coughing, during extubation. The present findings suggest that EA-Shield could prevent the exposure of aerosol to physicians and medical staff.

An infection barrier must be cheap, mass-producible, and single-use. EA-Shield has all these characteristics because it can be made using a 120-l clear plastic bag and double-sided tape. Our experiment was performed even in a non-negative pressurised room, and the results revealed that EA-Shield could provide protection against aerosols in non-negative pressurised rooms, including patient wards, operating rooms, and intensive care units. By using the EA-Shield, emergency airway management after extubation, including mask ventilation and oral suctioning, can be performed without modification. In clinical practice, it can be adapted to

the patient's body movements. Moreover, this shield was designed to allow effective ventilation inside using a fixed suction tube that creates a continuous negative pressure during the procedure (Video S1). After the patient's cough had subsided, he was made to wear a mask before the shield was removed. However, we believe that it is better to wear PPE because the Hasegawa method needs to be validated in clinical practice and has not been tested for exposure during discarding.

Although particle counting can provide numerical and objective assessment, it provides fixed-point observations, because spatial assessment is not sufficient [15–17]. The volume aspirated during the measurement is small compared to space or ventilation, and particle counting is inevitably influenced by the direction of the inlet. Although visualisation assessments can easily determine the spatial and temporal dispersal of aerosols, it is difficult to obtain numerical and objective assessments from videography [18–20]. To provide a thorough evaluation of aerosol dispersal, we combined particle counting with these assessments.

In addition, we used two types of tracers. Titanium dioxide particles have a wide range of diameters [21,22], whereas micron oil has good flowability for air movement [18–20]. The aerosol particles have a wide range of diameters (0.01–100 μm); therefore, it is difficult to assess the dispersal of these particles of all sizes, at once. Therefore, we measured the wind vector with micron oil, which has good tracking of air movement [23–25]. Measurement of the wind

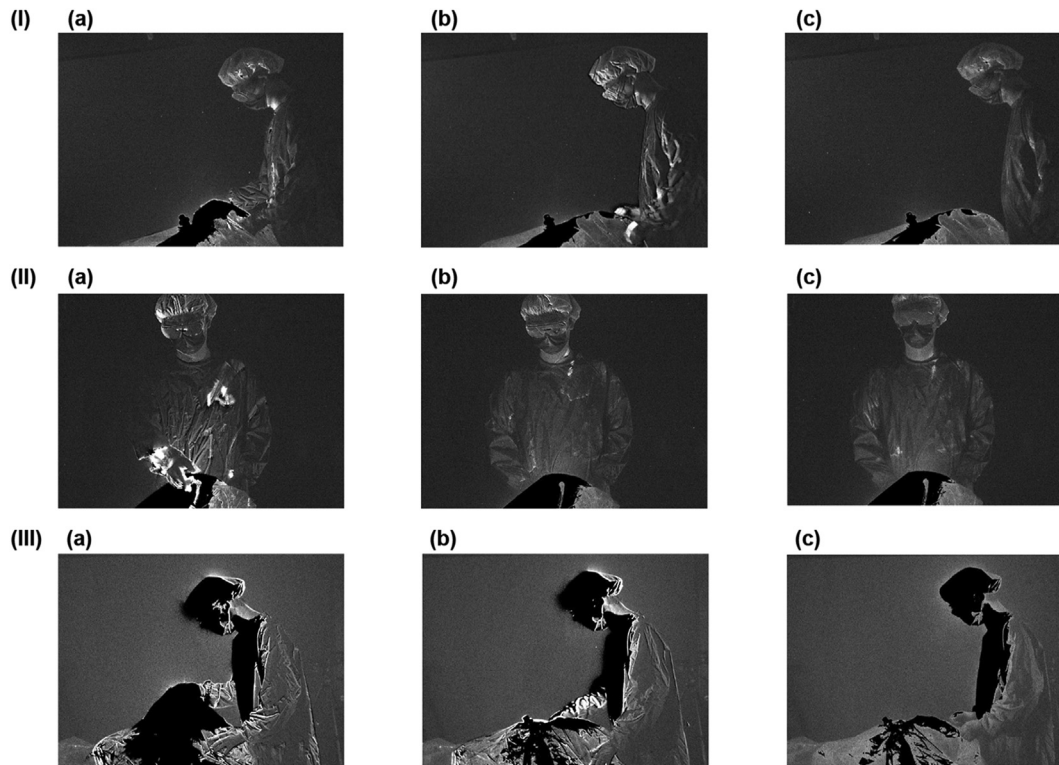


Figure 4. Photography of aerosol dispersal for 3, 5, and 10 s after the cough simulation with white LED light and green slit-sheet light in group H. (I) Photography with white LED light (three-dimensional assessment), (II) photography with green slit-sheet light in a sagittal view, and (III) photography with green slit-sheet light in an axial view (two-dimensional assessment from two directions). Aerosol dispersal is shown at (a) 3 s, (b) 5 s, and (c) 10 s after the cough simulation. In group H, there was no aerosol dispersal at 3, 5, or 10 s after extubation.

vector provided information regarding the dispersal of aerosol particles having small diameters ($<0.3 \mu\text{m}$, which are invisible with a CCD camera) [26]. Particles $0.3 \mu\text{m}$ in diameter or larger could be assessed using titanium dioxide, particle counting, and visualisation assessments. Therefore, the combination of titanium dioxide and micron oil provides information regarding the dispersal of aerosol particles of all sizes.

Our videography showed that EA-Shield could completely prevent aerosol exposure to the physician as well as in the surrounding area. It could protect the medical staff who stand by the patient as well as the instruments from aerosol exposure during extubation.

We used two-dimensional and three-dimensional high-quality videography for visualisation assessments. Our results revealed that EA-Shield completely prevented aerosol dispersal. Although small particles ($>0.3 \mu\text{m}$) can be detected using two-dimensional videography with the green slit-sheet light detects, spatial assessment is not sufficient because the laser-sheet light scatters only the particles on the laser line [18–20]. In addition, videography using a green slit-sheet laser has better quality than videography using other light sources because it is not easily affected by reflection. We used a green slit-sheet laser from two directions and assessed sagittal and axial aerosol dispersal. Measurement of the maximum distance

and area of aerosol dispersal for 3, 5, and 10 s after cough simulation using green slit-sheet light could provide numerical and objective assessments [18–20].

This is the first study that assesses three-dimensional aerosol dispersal using white LED light. Three-dimensional visualisation assessment using white LED light enables more detection of spatial and temporal aerosol dispersal than two-dimensional visualisation assessment. However, because white LED light is a wide-angle strong light source, reflection must occur, and numerical assessment may be difficult. The combination of two-dimensional and three-dimensional visualisation assessments can provide numerical, spatial, and temporal information on aerosol dispersal. According to the results obtained using a particle image velocimetry system, EA-Shield could prevent the generation of wind after extubation. It is therefore possible that EA-Shield can prevent transmission of aerosols and droplets as well as particles smaller than aerosols. A particle image velocimetry system has been used to assess aerosol dispersal from cough and cough parameters in several studies [23–25]. One study showed that the wind parameter determined by using a particle image velocimetry system enabled the assessment of the dispersal of aerosol particles with particles of small diameters [27]. The present results showed that using a face mask could not prevent exposure of the physician to aerosol

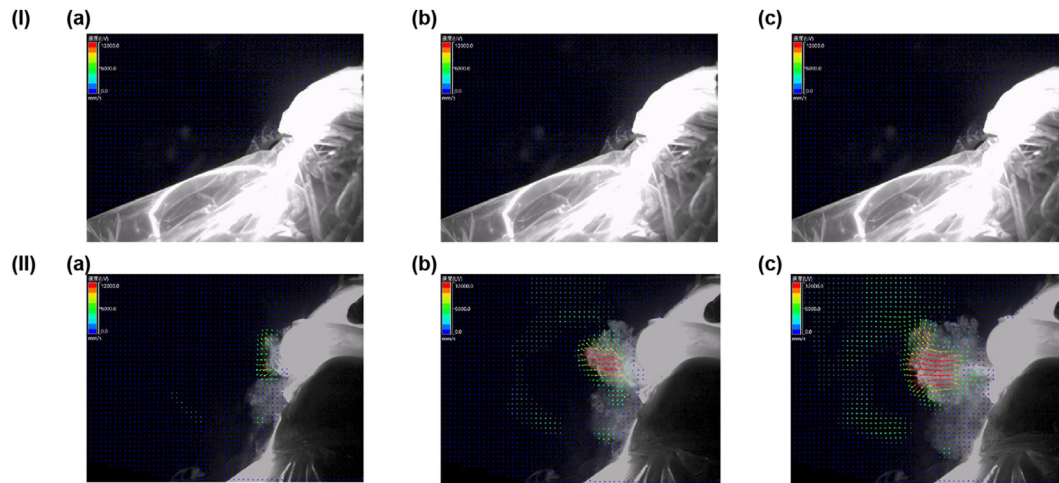


Figure 5. Wind vectors determined using the particle imaging velocimetry system. The movement of scattered particles illuminated by the green laser sheet was recorded automatically just before extubation to 15 s after extubation using image processing software (FlowExpert2D2C, Kato Koken) with a particle image velocimetry system, to which the successive abandonment method was applied for improvement. The movement of particles was changed to vectors with colour graduation based on their velocity levels via this software. The reference area was set as 640×480 pixels to 18.7×14.0 cm. The maximum error in the measurement of the velocity vector was estimated to be 0.23 m/s in our model. There was no wind at 0.3, 0.5, or 1 s after extubation in group H. In contrast, in group M, the wind was emitted from the space between the face mask and the mannequin's mouth after extubation, and the wind vectors were mainly to the right of the mannequin. (I) Group H and (II) group M. Wind vectors are shown at (a) 3 s, (b) 5 s, and (c) 10 s after the cough simulation.

particles, during extubation. Therefore, using this method could be a mistake. The Hasegawa method is highly reproducible and can be used by anyone. The results of the vector analysis revealed that this method accelerated the wind speed of the cough. This acceleration was caused by the narrow space between the face of the mannequin and the face mask compared to the mannequin's mouth, that could increase aerosol dispersal during extubation. Large aerosol particles (60–100 μm in diameter) have been found to be > 2 m with a velocity of 10 m/s recorded at the exit point [28,29]. Using a face mask could generate dispersal of the aerosols at more than 10 m/s during extubation; therefore, the medical staff must maintain a distance of at least 2 m from the patient.

In addition, an assistant is required for the physician during extubation; therefore, the face mask method increases the number of persons who could be exposed to aerosols, which does not obey the principle of aerosol protection. Moreover, the results obtained using the present particle image velocimetry system showed that the face mask method could generate turbulence. Turbulence is buoyant, increasing the aerosol dispersal and allowing the aerosolised particles to float in the air for a long time [30]. In contrast, the EA-Shield is an aerosol barrier that does not generate turbulence during extubation.

Although we used two tracers in our experiment, the aerosol dispersal determined by our tracers would not be the same as the actual aerosol dispersal after extubation. In addition, in a clinical situation, the patient can move during extubation, and the direction of the cough and aerosol dispersal can be altered. Moreover, aerosol dispersal can be changed by environmental factors including atmospheric pressure, room wind, temperature, humidity, and room size, as well as by movement factors, including those of medical staff around the patient [31–34]. We conducted our experiment with a trained

physician in a quiet room. Therefore, clinicians must consider how they can utilise the present results to obtain individual protection from aerosol dispersal.

Conclusions

EA-Shield, which can be crafted with common items, protects the physician against aerosol exposure during extubation. Therefore, we recommend using EA-Shield during extubation as an aerosol barrier when the risk of infectious aerosols is suspected.

Credit author statement

Gen Hasegawa: Conceptualization; Methodology; Data curation; Writing original draft.

Wataru Sakai: Conceptualization; Methodology; Data curation; Writing original draft.

Tomohiro Chaki: Validation; Formal analysis; Writing review and editing.

Shunsuke Tachibana: Validation; Formal analysis; Writing review and editing.

Atsushi Kokita: Conceptualization; Methodology; Data curation.

Takenori Kato: Data curation; Visualization; Supervision.

Hidekazu Nishimura; Writing review and editing; Supervision.

Michiaki Yamakage; Writing review and editing; Supervision; Funding acquisition.

Acknowledgements

We would like to thank Kouya Mikami of Kato Koken, Isehara, Japan, for their help with the experiments.

Conflict of interest statement

Authors declare no conflict of interest.

Funding sources

None.

Appendix A. Supplementary data

Supplementary data to this article can be found online at <https://doi.org/10.1016/j.infpip.2021.100193>.

References

- [1] Brown J, Gregson FKA, Shrimpton A, Cook TM, Bzdek BR, Reid JP, et al. A quantitative evaluation of aerosol generation during tracheal intubation and extubation. *Anaesthesia* 2021;76:174–81.
- [2] Yu X, Yang R. COVID-19 transmission through asymptomatic carriers is a challenge to containment. *Influenza Other Respir Viruses* 2020;14:474–5.
- [3] Stewart CL, Thornblade LW, Diamond DJ, Fong Y, Melstrom LG. Personal protective equipment and COVID-19: a review for surgeons. *Ann Surg* 2020;272:e132–8.
- [4] Cook TM, Lennane S. Occupational COVID-19 risk for anaesthesia and intensive care staff - low-risk specialties in a high-risk setting. *Anaesthesia* 2021;76:295–300.
- [5] Smither SJ, Eastaugh LS, Findlay JS, Lever MS. Experimental aerosol survival of SARS-CoV-2 in artificial saliva and tissue culture media at medium and high humidity. *Emerg Microbes Infect* 2020;9:1415–7.
- [6] Cook TM, El-Boghdady K, McGuire B, McNarry AF, Patel A, Higgs A. Consensus guidelines for managing the airway in patients with COVID-19: Guidelines from the Difficult Airway Society, the Association of Anaesthetists the Intensive Care Society, the Faculty of Intensive Care Medicine and the Royal College of Anaesthetists. *Anaesthesia* 2020;75:785–99.
- [7] Brewster DJ, Chrimes N, Do TB, Fraser K, Groombridge CJ, Higgs A. Consensus statement: Safe Airway Society principles of airway management and tracheal intubation specific to the COVID-19 adult patient group. *Med J Aust* 2020;212:472–81.
- [8] Orser BA. Recommendations for endotracheal intubation of COVID-19 patients. *Anesth Analg* 2020;130:1109–10.
- [9] Fennelly KP. Particle sizes of infectious aerosols: implications for infection control. *Lancet Respir Med* 2020;8:914–24.
- [10] D'Silva DF, McCulloch TJ, Lim JS, Smith SS, Carayannis D. Extubation of patients with COVID-19. *Br J Anaesth* 2020;125:e192–5.
- [11] Canelli R, Connor CW, Gonzalez M, Nozari A, Ortega R. Barrier enclosure during endotracheal intubation. *N Engl J Med* 2020;382:1957–8.
- [12] Asenjo JF. Safer intubation and extubation of patients with COVID-19. *Can J Anaesth* 2020;67:1276–8.
- [13] Sakai W, Tachibana S, Yamakage M. Cross-holes on a plastic bag can prevent droplet spread during extubation. *Anesth Analg* 2020;131:e189–91.
- [14] Kache S, Chisti MJ, Gumbo F, Mupere E, Zhi X, Nallasamy K. COVID-19 PICU guidelines: for high- and limited-resource settings. *Pediatr Res* 2020;88:705–16.
- [15] Simpson JP, Wong DN, Verco L, Carter R, Dzidowski M, Chan PY. Measurement of airborne particle exposure during simulated tracheal intubation using various proposed aerosol containment devices during the COVID-19 pandemic. *Anaesthesia* 2020;75:1587–95.
- [16] Lang AL, Shaw KM, Lozano R, Wang J. Effectiveness of a negative-pressure patient isolation hood shown using particle count. *Br J Anaesth* 2020;125:e295–6.
- [17] Fidler RL, Niedek CR, Teng JJ, Sturgeon ME, Zhang Q, Robinowitz DL, et al. Aerosol retention characteristics of barrier devices. *Anesthesiology* 2021;134:61–71.
- [18] Hui DS, Hall SD, Chan MT, Chow BK, Ng SS, Gin T, et al. Exhaled air dispersion during oxygen delivery via a simple oxygen mask. *Chest* 2007;132:540–6.
- [19] Hui DS, Chow BK, Lo T, Tsang OTY, Ko FW, Ng SS, et al. Exhaled air dispersion during high-flow nasal cannula therapy versus CPAP via different masks. *Eur Respir J* 2019;53:1802339.
- [20] Hui DS, Hall SD, Chan MT, Chow BK, Tsou JY, Joynt GM, et al. Noninvasive positive-pressure ventilation: An experimental model to assess air and particle dispersion. *Chest* 2006;130:730–40.
- [21] Pujalté I, Serventi A, Noël A, Dieme D, Haddad S, Bouchard M. Characterization of aerosols of titanium dioxide nanoparticles following three generation methods using an optimized aerosolization system designed for experimental inhalation studies. *Toxics* 2017;5:14.
- [22] Noël A, Cloutier Y, Wilkinson KJ, Dion C, Hallé S, Maghni K, et al. Generating nano-aerosols from TiO₂ (5 nm) nanoparticles showing different agglomeration states. Application to toxicological studies. *J Occup Environ Hyg* 2013;10:86–96.
- [23] Chao CYH, Wan MP, Morawska L, Johnson GR, Ristovski ZD, Hargreaves M, et al. Characterization of expiration air jets and droplet size distributions immediately at the mouth opening. *J Aerosol Sci* 2009;40:122–33.
- [24] Kwon SB, Park J, Jang J, Cho Y, Park DS, Kim C, et al. Study on the initial velocity distribution of exhaled air from coughing and speaking. *Chemosphere* 2012;87:1260–4.
- [25] Pantelic J, Tham KW, Licina D. Effectiveness of a personalized ventilation system in reducing personal exposure against directly released simulated cough droplets. *Indoor Air* 2015;25:683–93.
- [26] Gomi K, Nagahama M, Yoshida E, Takano Y, Kuroki Y, Yamamoto Y. Peroral endoscopy during the COVID-19 pandemic: Efficacy of the acrylic box (Endo-Splash Protective (ESP) box) for preventing droplet transmission. *JGH Open* 2020;4:1224–8.
- [27] Nishimura H, Sakata S, Kaga A. A new methodology for studying dynamics of aerosol particles in sneeze and cough using a digital high-vision, high-speed video system and vector analyses. *PLOS ONE* 2013;8:e80244.
- [28] Wells WF. On air-borne infection: study II. Droplets and droplet nuclei. *Am J Epidemiol* 1934;20:611–8.
- [29] Xie X, Li Y, Chwang AT, Ho PL, Seto WH. How far droplets can move in indoor environments-revisiting the Wells evaporation-falling curve. *Indoor Air* 2007;17:211–25.
- [30] Bourouiba L, Dehandshoewercker E, Bush JWM. Violent respiratory events: on coughing and sneezing. *J Fluid Mech* 2014;745:537–63.
- [31] Vuorinen V, Aarnio M, Alava M, Alopaeus V, Atanasova N, Auvinen M, et al. Modelling aerosol transport and virus exposure with numerical simulations in relation to SARS-CoV-2 transmission by inhalation indoors. *Saf Sci* 2020;130:104866.
- [32] Tang JW, Li Y, Eames I, Chan PK, Ridgway GL. Factors involved in the aerosol transmission of infection and control of ventilation in healthcare premises. *J Hosp Infect* 2006;64:100–14.
- [33] Elazhary MA, Derbyshire JB. Effect of temperature, relative humidity and medium on the aerosol stability of infectious bovine rhinotracheitis virus. *Can J Comp Med* 1979;43:158–67.
- [34] Bello A, Quinn MM, Perry MJ, Milton DK. Quantitative assessment of airborne exposures generated during common cleaning tasks: a pilot study. *Environ Health* 2010;9:76.